Pergamon

Int. J. Solids Structures Vol. 33, No. 13, pp. 1837–1851, 1996

0020-7683/96 $15.00 + .00

0020-7683(95)00133-6

CIRCUMFERENTIAL STIFFENERS AS BUCKLE ARRESTORS IN LONG PANELS

T. L. POWER and S. KYRIAKIDES
Engineering Mechanics Research Laboratory, Department of Aerospace Engineering and Engineering Mechanics, The University of Texas at Austin, Austin, Texas 78712, U.S.A.

(*Received* 9 *February* 1995; *in revised form* 22 *May* 1995)

Abstract—It is well known that certain larger structures are susceptible to a type of collapse which starts locally but under favorable conditions can spread and has the potential of affecting the whole structure. The lowest load which can sustain this spreading of collapse (*propagation load*) is usually significantly lower than the critical buckling load of the geometrically intact structure. As a result, the option of avoiding the potentiality of propagating collapse by using the propagation load as the design criterion can result in significant penalties in cost and weight. An alternative is to base the design on the critical buckling load of the structure while including periodic stiffeners to arrest potential propagating collapse and keep its effect local. This paper illustrates this new design philosophy through an example involving a long pressure-loaded panel with sparsely spaced circumferential stiffeners cast in the role of buckle arrestors. An analysis is presented which models the process of quasi-static buckle penetration through such a stiffener. A general measure of arresting performance is defined, based on the maximum pressure experienced during the penetration process. A general framework for establishing the dependence of the stiffener arresting efficiency on the problem parameters is developed. Furthermore, fundamental concepts regarding limiting values for stiffener length and thickness are introduced, and results are presented which indicate that in this problem short, thick stiffeners provide the most arresting capacity for a given amount of stiffener material.

INTRODUCTION

Recently, it has been demonstrated that the onset of global instability in long, pressure-loaded, cylindrical panels is followed by localized collapse which affects only a section a few panel spans long (see Power and Kyriakides, 1994). This collapse, once initiated, can propagate along the panel at pressures well below the pressure at which a geometrically perfect panel first becomes unstable. Under prescribed pressure conditions, the collapse will spread dynamically over the entire structure unless the collapse fronts encounter obstruction. The lowest pressure at which collapse can propagate is usually only a fraction of the pressure required to initiate the instability. Consequently, designing the entire structure against propagating collapse may not be feasible for reasons of excessive weight or cost. An alternative design philosophy is to ensure that collapse, should it occur, remains local. Periodic placement of circumferential stiffeners along the structure can provide the necessary containment by constraining the collapse to remain within the region bounded by the two stiffeners on either side of the initiation site.

The usual motivation for the use of stiffeners in shell structures is to increase their resistance to buckling. By contrast, in this work, we examine the behavior of structures which have already experienced local collapse, where the purpose of the stiffeners is to arrest the spreading of this collapse to the rest of the structure. The design issues then are the selection of the most effective and efficient stiffener and the determination of the optimum spacing between adjacent stiffeners. The characteristics of this new class of problems are illustrated below in examples involving shallow cylindrical panels under external pressure. In this first treatment of the problem, attention will be limited to quasi-static propagation and arrest of such instabilities.

One of the examples analyzed in the preceding paper involved a long shallow cylindrical panel with a circular arch cross section and a shallowness parameter

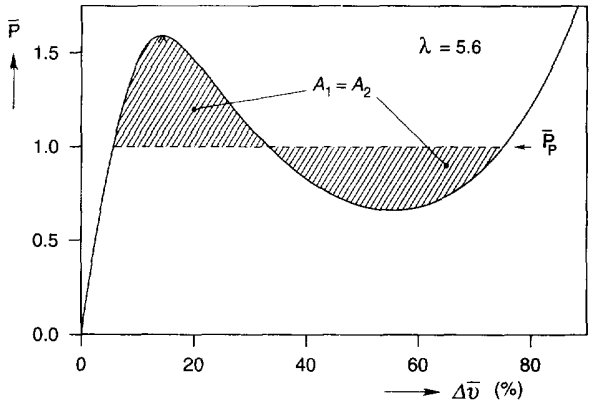

Fig. 1. Pressure-displaced volume response for panel collapsing uniformly along its length.

$$\lambda = \alpha^2 \frac{R}{t} = 5.6 \tag{1}$$

where 2α is the arch span angle, R its radius, and t its wall thickness. The pressure-displaced volume ($P-\Delta v$) response of a long linearly elastic panel of this geometry, constrained to be collapsing uniformly along its length (plane strain), is shown in Fig. 1. It has the *up–down–up* characteristic shape of the response of the corresponding one-dimensional arch, and it can be derived from the arch solution by replacing Young's modulus with the appropriate plane strain modulus. It was shown, however, that by contrast, in the case of the panel, only the first ascending part of this response is stable. Beyond the pressure maximum, axially nonuniform deformation modes become energetically preferable and the actual global response departs radically from the axially uniform response as the collapse localizes.

Figure 2a shows the quasi-static $P-\Delta v$ response calculated for a panel which is 20 spans long ($2L = 20S$). The localized nature of the deformation following the limit load can be seen in the calculated deformed configurations shown in Fig. 2b. Eventually, tensile membrane stresses develop in the collapsed section which cause further lateral deformation to be arrested. At this stage, spreading of the collapse to the rest of the structure becomes preferable with the transition region between the collapsed and uncollapsed regions acting as a destabilizing agency on the uncollapsed section. Under the loading conditions of this simulation, the propagation of collapse quickly reaches a steady state represented by the pressure plateau in Fig. 2a. This represents the lowest pressure at which a buckle will propagate under any conditions, termed the *propagation pressure* (P_P) of the structure. For elastic panels, the propagation pressure can be determined exactly from the plane strain $P-\Delta v$ response of the panel by conducting a steady-state energy balance analysis of the quasi-static propagation process. This calculation yields P_P as the pressure which makes the two shaded areas in Fig. 1 equal (known as the *Maxwell construction*; see Ericksen, 1975; Chater and Hutchinson, 1984; and Kyriakides, 1993). If the plane strain response is calculated by using the lowest order admissible nonlinear kinematics (Schreyer and Masur, 1966), the propagation pressure is given by the following (Kyriakides and Arseculeratne, 1993):

$$P_P = \frac{1}{12} \frac{E}{(1-\nu^2)} \left(\frac{\pi}{\alpha}\right)^2 \left(\frac{t}{R}\right)^3 \tag{2}$$

where E is the Young's modulus and ν the Poisson's ratio of the panel material. The collapse will continue to propagate at this pressure until either the whole structure is collapsed or the collapse front encounters an obstacle in its path. In what follows, we examine the effectiveness of circumferential stiffeners as arrestors of propagating collapse in such panels.

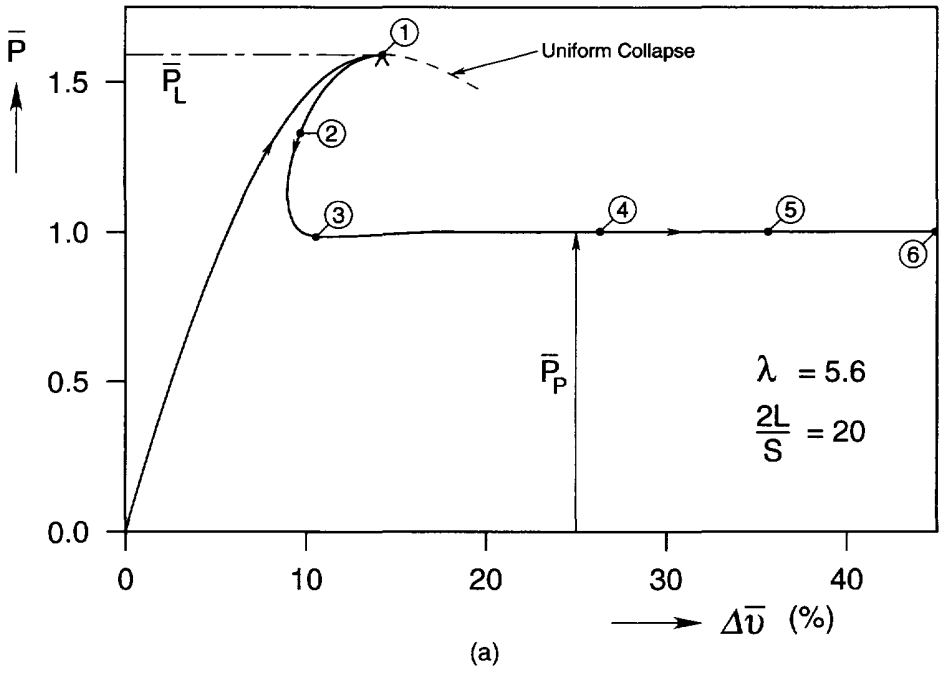

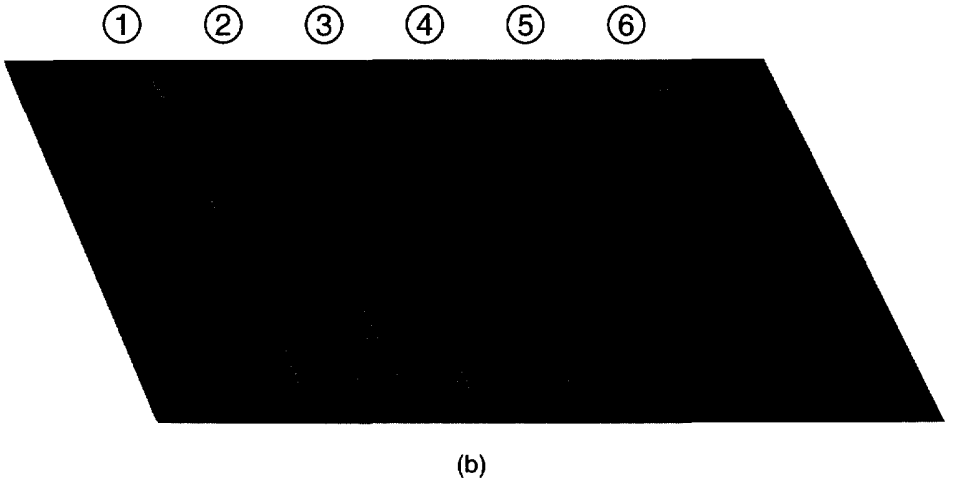

Fig. 2. Unstiffened panel analysis (a) actual (localizing) quasi-static pressure-displaced volume response for long shallow panel; (b) sequence of calculated configurations.

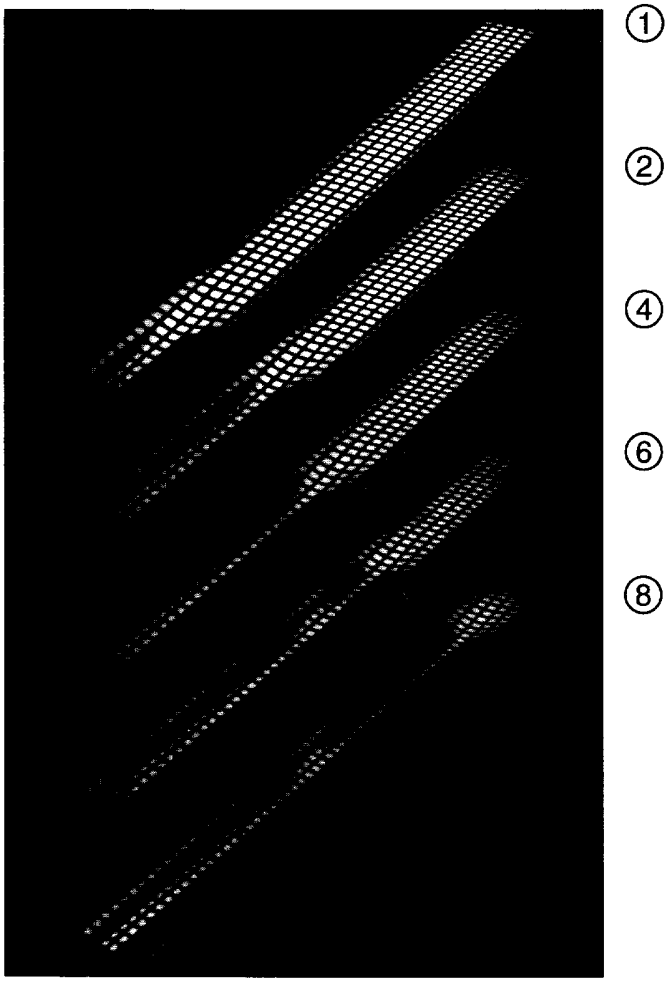

Fig. 4c.

ANALYSIS

We consider a long circular cylindrical panel of radius R, span angle 2α, and wall thickness $t(\ll R)$ loaded by uniform external pressure P. The panel is reinforced with circumferential stiffeners placed a distance L apart whose sole purpose is to limit the extent of collapse in the event that a buckle is accidentally initiated in the structure. Because of this limited objective, they are placed relatively far apart and therefore have no significant influence on the collapse pressure of the panel. Due to the periodicity of the structure, we limit attention to the section shown in Fig. 3 with overall length $2L$. This section contains two circumferential stiffeners, each of length L_s and thickness h, arranged symmetrically with respect to the plane $x_1 = 0$. Each stiffener is modeled as a thickened region with the same midsurface radius R as the remainder of the panel. The panel material is taken to be linearly elastic with properties E and ν defined above. Without loss of generality, collapse will be initiated so that it is symmetric about the plane $x_1 = 0$, and we assume that subsequent deformation will maintain this symmetry. In this work, we consider only panels with low enough values of λ so that deformations remain symmetric about the midspan. Thus, the plane $x_2 = 0$ is taken as an additional plane of symmetry, and only the region $[0 \leqslant x \leqslant L,\ 0 \leqslant \theta \leqslant \alpha]$ is analyzed. Axial, circumferential, and radial displacement components are denoted by u, v, and w, respectively.

The nonlinear shell kinematics (Sanders, 1963) used in the analysis are given in Appendix A. The structure was discretized by assuming admissible series expansions for the displacements which appear in Power and Kyriakides (1994). The displacement expansions satisfy fully fixed conditions on the boundaries $\theta = \pm\alpha$ and exhibit symmetry in both x and θ. In addition, the slope $w_{,x}$ vanishes at the boundaries $x = \pm L$. For more details on discretization and on numerical convergence issues, see Power (1995).

Equilibrium of the structure is enforced through the principle of virtual work, which for uniform lateral pressure loading may be expressed as follows:

$$\int\int_A [N_{\alpha\beta}\delta E_{\alpha\beta} + M_{\alpha\beta}\delta K_{\alpha\beta}]\,\mathrm{d}A = P\delta\Delta v \tag{3}$$

where $N_{\alpha\beta}$ and $M_{\alpha\beta}$ are the force and moment intensities, related to $E_{\alpha\beta}$ and $K_{\alpha\beta}$ through the

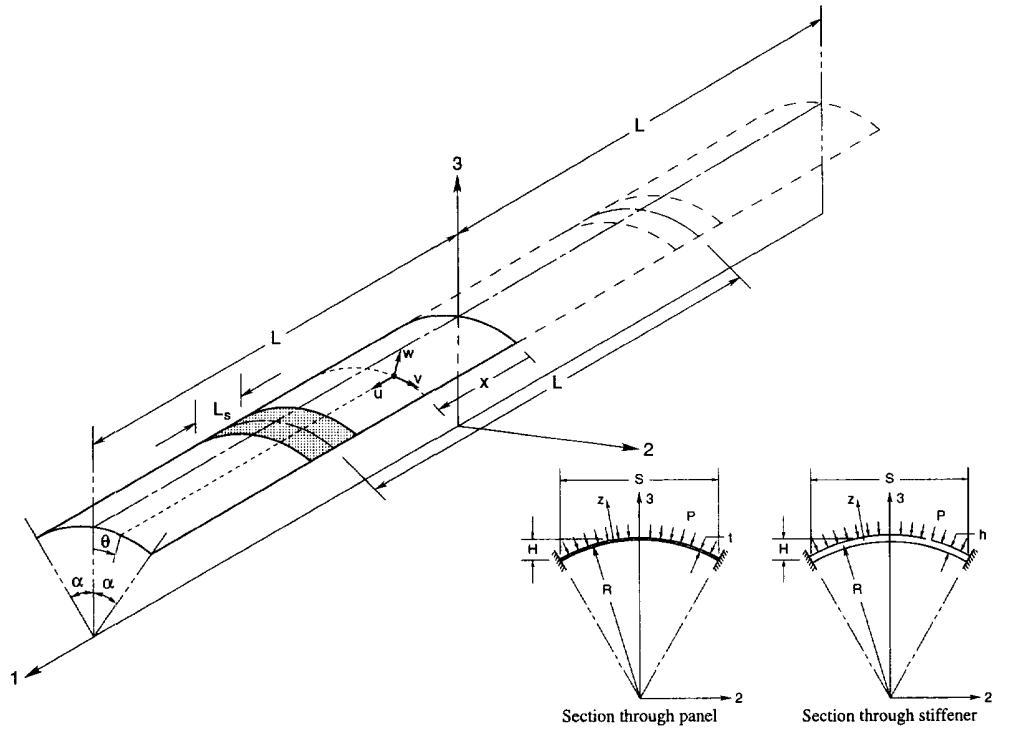

Fig. 3. Geometry of analyzed panel.

usual isotropic linearly elastic relationships (surface integrations are performed by Gaussian quadrature over the part of the panel analyzed—see Fig. 3). The thickness value used in these constitutive equations is h for material points within a stiffener, and t for points in the remainder of the panel. The volume displaced from underneath the panel, Δv, is given by

$$\Delta v = -\int\int_A \left[w + \tfrac{1}{2}(wu_{,x} - w_{,x}u) + \frac{1}{2R}(w^2 + wv_{,\theta} - w_{,\theta}v + v^2) \right] \mathrm{d}A \tag{4}$$

(see also Dyau and Kyriakides, 1993).

The panel is loaded incrementally using an arc length procedure similar to that proposed by Riks (1979) (see Power, 1995). Since the complexities associated with the initiation and localization of collapse are not of interest in this study, the analysis is begun at a deformed configuration in the steady-state propagation regime. This configuration is found by using a deformed configuration in the steady-state regime from an analysis of an unstiffened panel as an initial guess for the corresponding stiffened panel solution, which is then obtained by Newton-Raphson iteration. After converging to this initial configuration, the arc length scheme is used to step along the quasi-static equilibrium path. This method of incrementation was chosen because of its ability to continue uninterrupted through turning points in the solution with respect to the usual physical control parameters. In this fashion, the solution process is fully automated after the first step.

RESULTS AND DISCUSSION

a. Penetration of a stiffener by a propagating buckle

The penetration of a propagating collapse front through a circumferential stiffener will be first illustrated by way of an example with $\lambda = 5.6$, $L_s/S = 1$, and $h/t = 1.16$. In this as

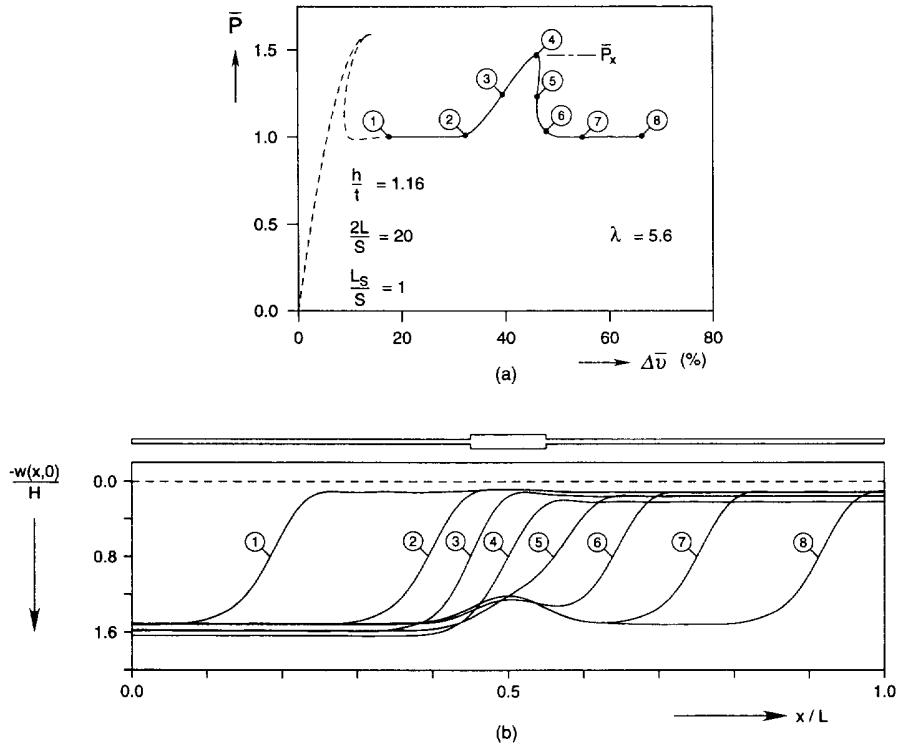

Fig. 4. Stiffened panel analysis: $L_s = S$ (a) pressure-displaced volume response; (b) deformed ridgeline configurations; (c) sequence of calculated configurations showing buckle penetration through stiffener (displacements amplified 3 ×).

well as in all subsequent examples, the panels analyzed have $R/t = 480$. Throughout this paper pressure and displaced volume are normalized as follows:

$$\bar{P} = \frac{P}{\frac{E}{12(1-\nu^2)}\left(\frac{\pi}{\alpha}\right)^2\left(\frac{t}{R}\right)^3} \quad \text{and} \quad \Delta\bar{v} = \frac{1}{\alpha^3}\frac{\Delta v}{R^2 L}. \tag{5}$$

The calculated pressure-displaced volume response is shown in Fig. 4a and a series of profiles of the deformed panel ridgeline (generator $\theta = 0$) at various stages of the response are shown in Fig. 4b (each profile corresponds to a point on the $\bar{P}-\Delta\bar{v}$ response as indicated with the circled numbers). The schematic diagram atop the profiles shows the axial location and extent of the circumferential stiffener. In addition, three-dimensional views of several of the deformed configurations are shown in Fig. 4c where the extent of the stiffener is identified by arrowheads.

In a structure like this one, initial collapse is local and can result from overloading due to impact by a foreign object or from other off-design loading conditions that can develop. Once initiated, the collapse propagates in both directions along the panel until it encounters the stiffeners. In this example, the quasi-static initiation process was also simulated and is shown in Fig. 4a with a dashed line. Because the stiffeners are positioned far enough apart from each other, the collapse initiates at almost the same pressure as for the corresponding unstiffened panel (difference less than 0.01%). Subsequently, the collapse localizes much like it did in the unstiffened example in Fig. 2. This, of course, is one way of getting to configuration ①.

From point ① to point ② of the response, the collapse propagates at the propagation pressure of the panel and the shape of the buckle front remains unchanged. We note from the profiles that, from point ① onward, the deformed configuration always consists of a collapsed section, an uncollapsed section, and a transition region joining the two. The collapsed and uncollapsed sections are axially uniform except in the vicinity of the stiffener. The presence of the stiffener first becomes apparent near point ② in the response. Due to the higher stiffness of the stiffener, an increase in pressure is required in order to continue the deformation of the structure. Indeed, if the pressure is not increased, the buckle will remain stationary (*arrested*). Initially, the stiffener deformation is relatively small and the main effect of the rising pressure is a steepening of the buckle front (e.g., see configuration ③) accompanied by a downward movement of the uniform collapsed and uncollapsed sections (notice the downward translation of the straight ridgeline sections from their positions during steady-state propagation). As the pressure is increased further, collapse gradually penetrates the stiffener until, at configuration ④, the front of the transition region has reached the far edge of the stiffener. At this point, a pressure maximum develops, and the last portion of the stiffener begins to collapse. The value of this maximum pressure is a measure of the effectiveness of the stiffener as an arrestor of propagating collapse and is known as the *crossover pressure* P_x (see Kyriakides and Babcock, 1980).

The subsequent decrease in pressure (④–⑦) causes elastic unloading in the uniform sections as illustrated by the return of the uniform ridgeline sections to their earlier positions corresponding to P_P. By point ⑦ in the response, the buckle front has passed the stiffener, and has resumed steady-state propagation at the propagation pressure. Because of its higher stiffness, the collapsed stiffener behind the buckle front appears in Fig. 4b and 4c as a hump in the collapsed panel.

It is of interest to note that as the stiffener collapses, the displaced volume Δv decreases during a portion of the equilibrium path in the neighborhood of configuration ⑤. This indicates that the rate at which volume is being displaced by the advancing collapse front is temporarily exceeded by the rate at which volume is being recovered underneath the axially uniform portions of the panel which unload in response to the pressure decrease. This turning point with respect to the displaced volume implies that even under volume-controlled loading the stiffener will collapse dynamically bridging the turning point with the point corresponding to the same Δv directly below it in the $P-\Delta v$ response. The clear

implication for longer panels is that this reversal in displaced volume will be more severe, resulting in a more energetic dynamic snap. This is very similar to the situation during the localization of collapse in long panels which is responsible for the cusp-like nature of the response in the vicinity of first instability (see Power and Kyriakides, 1994).

A more detailed view of the deformation of the stiffener as it is being penetrated by the buckle front can be seen in Fig. 5. Figure 5a shows the pressure vs the displacement at the center of the stiffener, and Fig. 5b shows several deformed configurations of the stiffener ridgeline. In view of its fixed boundaries, lateral deflection causes twisting of the stiffener during the penetration process. It is also interesting to observe that configuration ⑤, which corresponds to the maximum pressure, is the configuration in which the buckle front has fully penetrated the stiffener for the first time in the sense that the right edge has just began to experience substantial rotation.

b. Design of stiffeners

A stiffener cast in the role described above is effective if it can arrest a buckle initiated at the maximum design load of the structure. In a constant pressure environment, the buckle front will engage the stiffener dynamically. If the pressurizing medium is a fluid, the problem will be further complicated by interaction between fluid flow and the motion of the structure. While these factors can be expected to influence the performance of such stiffeners used as buckle arrestors, it is helpful in establishing the relative importance of the problem parameters if the first evaluation of such devices is carried out in the simpler quasi-static setting. Moreover, it will be shown that certain practical limitations on these parameters become apparent in this setting. Realizing that the selection of a maximum design load is problem-specific and is the prerogative of the design engineer, we choose to describe a stiffener which resists penetration for all pressures between P_P and P_C as having maximum effectiveness (P_C is the critical global buckling pressure of the panel that is, either

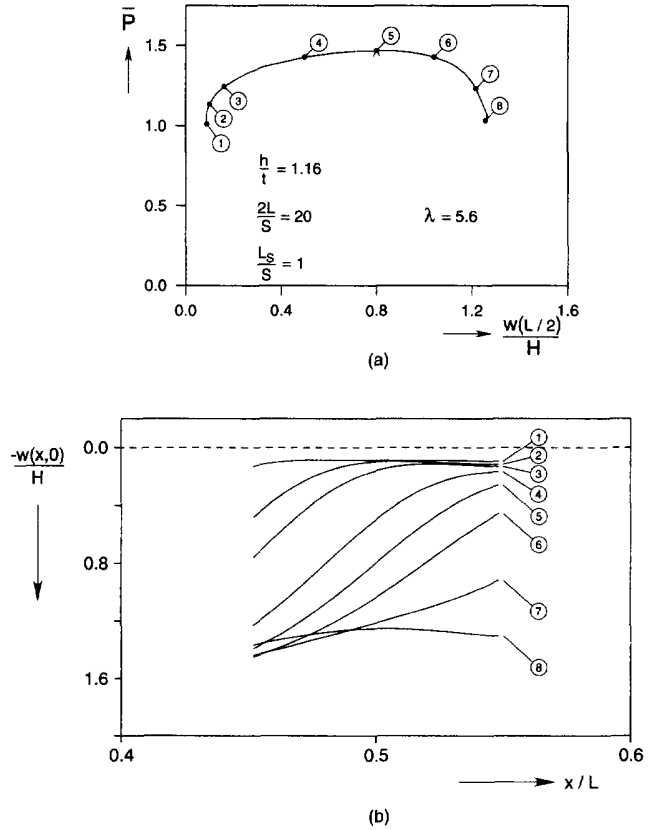

Fig. 5. Stiffener behavior during buckle penetration (a) pressure vs center displacement; (b) profiles of stiffener ridgeline.

the limit pressure P_L of the perfect response for shallower panels, or the bifurcation buckling pressure P_b for less shallow panels—see Power and Kyriakides, 1994). This, of course, is the highest demand that can be placed on an arrestor since crossover pressures higher than P_C cannot be realized in the problem as defined because of the incipient collapse of the unstiffened sections of the long panel. Based on this requirement, we define the following measure of buckle arresting efficiency η for the stiffener

$$\eta = \frac{P_x - P_P}{P_C - P_P} \tag{6}$$

so that $0 \leqslant \eta \leqslant 1$ (see also Kyriakides and Babcock, 1980). For example, the panel discussed in the previous section had a $\bar{P}_C = 1.591$ and the stiffener crossover pressure was $\bar{P}_x = 1.469$; thus according to eqn (6) the arresting efficiency of the stiffener is 0.794. In what follows, we examine the dependence of η on the stiffener geometric parameters h and L_s.

Effect of stiffener wall thickness. Similar calculations to the one presented in Fig. 4 were conducted for stiffeners one panel span long and of varying wall thickness. In the analyses that follow, we intentionally bypass the initiation process and begin the calculations with the buckle propagating quasi-statically toward both stiffeners at the propagation pressure of the panel. The calculated $P-\Delta v$ responses for seven such stiffened panels with $1.05 \leqslant h/t \leqslant 1.19$ are shown in Fig. 6. Increase of the stiffener wall thickness results in an increase in the crossover pressure and a corresponding increase in the arresting efficiency of the stiffener. Interestingly, for a stiffener of this length, a wall thickness just over 19% higher than that of the panel is sufficient to resist quasi-static buckle penetration up to the pressure $\bar{P}_L$. In other words, for $L_s = S$, the stiffener thickness necessary to yield an efficiency of 1.0 is $h = 1.196t$. We will refer to this as the *critical stiffener wall thickness* for this length and designate it by h_c.

As might be expected, the rising (stable) part of the $P-\Delta v$ response during the penetration process becomes steeper as the stiffener wall thickness is increased. After the limit load, the pressure returns sharply to the propagation pressure of the panel. For the stiffeners with lower wall thicknesses ($h/t = 1.05$, 1.10 and 1.12) in Fig. 6, this occurs at strictly increasing values of Δv. The four cases with higher h/t values, however, exhibit turning points with respect to Δv, indicating that even under volume-controlled loading, the penetration of such stiffeners by a buckle can be expected to involve a dynamic snap.

The arresting efficiency of this set of stiffeners ($L_s/S = 1$), based on the calculated crossover pressures, is plotted as a function of their wall thickness in Fig. 7. η is seen to be mildly nonlinearly related to h/t but the behavior is such as to suggest that the penetration process for shallow panels is primarily governed by membrane effects. Also included in Fig. 7 are similar sets of results for three shorter stiffeners ($L_s/S = 0.5$, 0.3 and 0.2). Clearly, as

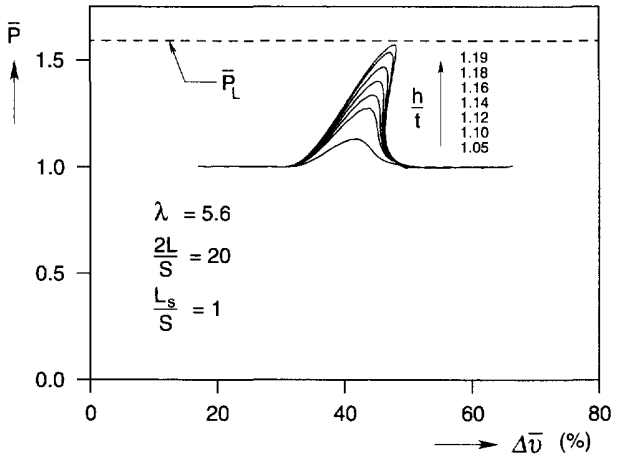

Fig. 6. Pressure-displaced volume responses for stiffened panels of various stiffener wall thickness.

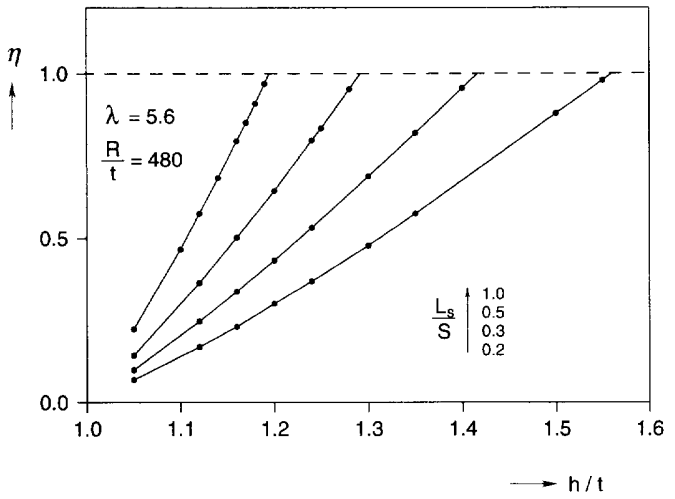

Fig. 7. Arresting efficiency as a function of stiffener wall thickness.

the length of the stiffener decreases, the wall thickness required in order to achieve a certain crossover pressure must increase. The mild nonlinearity in the relationship between η and h/t is present for all four stiffener lengths. The values of stiffener wall thickness required for the four cases to achieve an efficiency of 1.0 are approximately as follows:

$\frac{L_s}{S}$	$\frac{h_c}{t}$
1.0	1.196
0.5	1.292
0.3	1.416
0.2	1.557

Effect of stiffener length and the minimum thickness stiffener. It is instructive to also look at the arresting efficiency as a function of stiffener length. Figure 8 shows several sets of results of η vs stiffener length for values of wall thickness in the range $1.12 \leqslant h/t \leqslant 1.35$. In the case of the two higher wall thicknesses shown (h/t of 1.35 and 1.30), the efficiency is seen to be increasing approximately linearly with stiffener length. As the wall thickness is reduced to $1.24t$ and to $1.20t$, the dependence of η on L_s becomes progressively more nonlinear and L_s must increase significantly more to produce a given increase in arresting

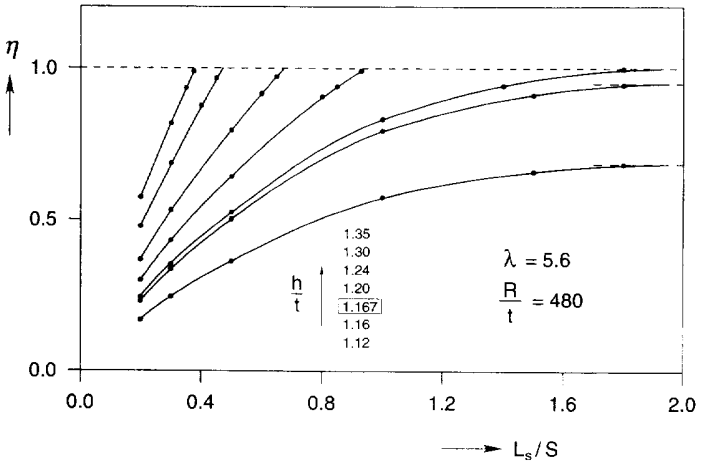

Fig. 8. Arresting efficiency as a function of stiffener length.

efficiency. In the case of $h/t = 1.12$ and 1.16 we observe that as the stiffener length increases, the efficiency approaches asymptotically the values of 0.686 and 0.951 respectively. That is, these are the maximum possible efficiencies that can be achieved with stiffeners of these wall thicknesses regardless of how long the stiffeners are made.

Clearly, there must be a particular value of h/t for which the asymptotic efficiency of long stiffeners is equal to 1.0. For the panel geometry considered in Fig. 8, this occurs at $h/t = 1.167$. We will refer to a stiffener with this wall thickness as the *minimum thickness stiffener* and designate its wall thickness as h_{cm}. This is the minimum thickness that a stiffener with an arresting efficiency of 1.0 can have, and it is a function of the geometry (α, R/t) of the panel. The simplest way of obtaining h_{cm} is as follows: Consider a buckle propagating quasi-statically in a given panel. Let it encounter a very long stiffener with the same mean radius R and span angle 2α as the panel. Use the expression of the propagation pressure in eqn (2) to evaluate the wall thickness h this long stiffener should have so that its own propagation pressure is equal to the critical global collapse pressure of the panel (P_C). In other words, ensure that such a stiffener will not develop a propagating buckle at a pressure lower than P_C. This condition is met when

$$h_{cm} = (\sqrt[3]{\bar{P}_C})t. \tag{7}$$

In the present panel example eqn (7) yields $h_{cm} = 1.1672t$.

The performance of several long stiffeners as buckle arrestors can be seen in the calculated $P-\Delta v$ responses shown in Fig. 9a. In these cases, one half of the length of the panels analyzed had a wall thickness t and the other half a wall thickness $h > t$. A buckle initiated in the thinner section propagates quasi-statically at the propagation pressure of the panel until it encounters the stiffened section(s). The buckle is then arrested and further deformation of the structure requires an increase in pressure. In each case, the pressure is seen to increase to a certain value and then remain constant as the buckle starts to propagate in the stiffener itself.

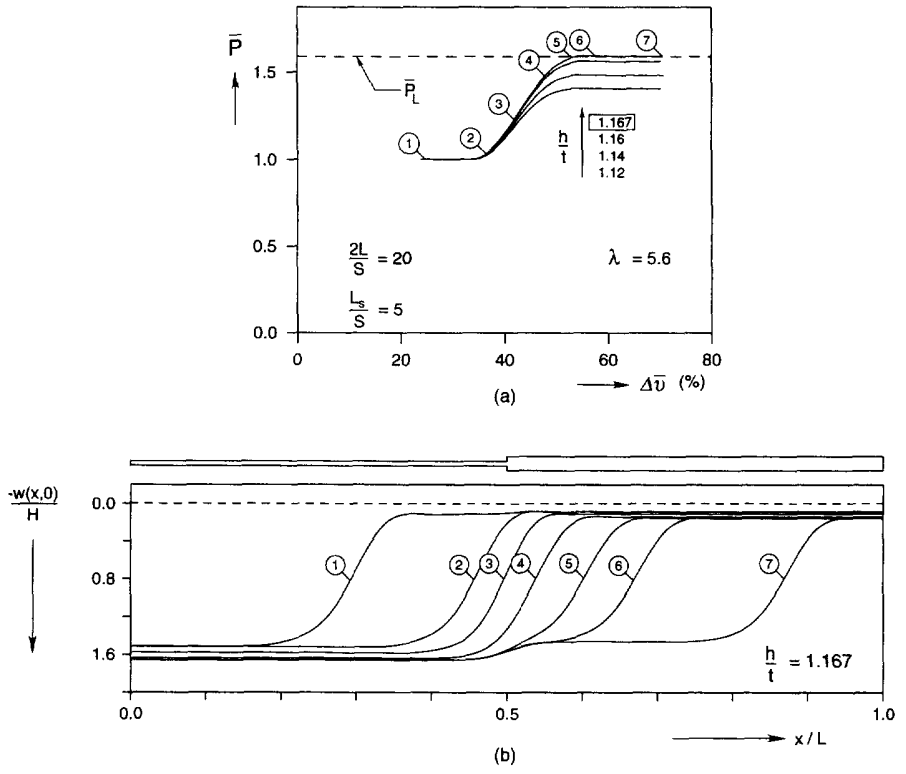

Fig. 9. Stiffened panel analysis: $L_s = 5S$ (a) pressure-displaced volume response; (b) deformed ridgeline configurations.

The case with $h/t = 1.1672$ is the minimum thickness stiffener for this panel. As a result, the level of the second pressure plateau reaches the level of the global collapse pressure of the unstiffened panel ($\bar{P}_L$); in other words, this stiffener is confirmed to have an arresting efficiency of 1.0 as predicted by the simpler calculation discussed earlier.

Figure 9b shows a sequence of deformed panel ridgelines during the penetration of this long minimum thickness stiffener by a propagating buckle. The deformed configurations correspond to the points on the $P-\Delta v$ response in Fig. 9a identified with the same number. Configuration ① shows the profile of a buckle propagating under steady-state conditions in the unstiffened part of the panel. Configurations ②–⑥ show the changes in the transition region profile during the penetration process. By configuration ⑦, a new steady state has been reached which involves quasi-static propagation of the buckle in the stiffener itself. As expected, the section of the panel which was collapsed earlier by a buckle propagating at a pressure of $\bar{P} = 1.0$ now deflects noticeably more due to the higher pressure. In Fig. 9b, this is indicated by the downward translation of the ridgeline in the thinner half. At the same time, the additional deflection of the ridgeline of the collapsed section of the thicker half is seen to be significantly smaller due to its higher wall thickness.

The $P-\Delta v$ responses corresponding to the three stiffeners with wall thickness less than h_{cm} are seen to have upper pressure plateaus which are progressively lower than $\bar{P}_L$. In each case, the pressure plateau yielded by the numerical calculation was found to correspond to the propagation pressure calculated using the appropriate value of thickness in eqn (2). An interesting observation from this set of four $P-\Delta v$ responses is that in all cases, the maximum value of pressure reached during the penetration process is the propagation pressure of the stiffener. Transient pressure peaks, characteristic of many other initiation mechanisms of propagating instabilities (see Kyriakides, 1993), are conspicuously absent. This behavior clearly implies that the maximum crossover pressure that can be achieved using stiffeners of these thicknesses is the propagation pressure of the stiffener.

A question of practical importance in the design of such stiffening devices is that of establishing the length at which a stiffener of finite length looks infinitely long to the buckle as far as its arresting efficiency is concerned. For the panel analyzed here, the answer to this question, for stiffeners required to have efficiency of 1.0, becomes evident from the plot of critical stiffener wall thickness versus the stiffener length shown in Fig. 10 (results cross plotted from Figs 7 and 8). For stiffeners shorter than $L_s/S = 1$, the critical wall thickness is seen to be strongly influenced by the stiffener length. For longer stiffeners the critical wall thickness asymptotically approaches the value of $h_{cm}/t = 1.1672$ (minimum thickness stiffener). In this case, a minimum thickness stiffener with a length of just $1.8S$ looks infinitely long to an incoming buckle. We will designate this minimum length for the minimum thickness stiffener by L_{sm}. Increase of the length of the stiffener beyond this value

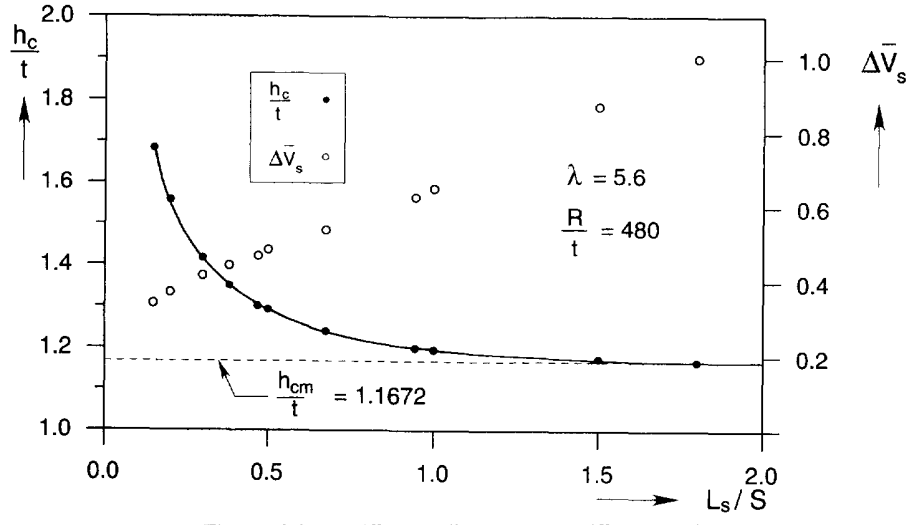

Fig. 10. Critical stiffener wall thickness vs stiffener length.

will result in no additional benefit to the structure, at least from the perspective of arresting buckles propagating quasi-statically. It is interesting to observe from the results in Fig. 8 that the two thinner stiffeners analyzed (h/t of 1.16 and 1.2) developed their maximum arresting efficiencies at approximately the same length as the minimum thickness stiffener.

For completeness, in Fig. 10 we include a plot of the additional volume of material required by each critical thickness stiffener as a function of its length where the normalized measure of material volume is defined as follows:

$$\Delta \bar{V}_s = \frac{L_s\left(\frac{h_c}{t} - 1\right)}{L_{sm}\left(\frac{h_{cm}}{t} - 1\right)}. \tag{8}$$

In spite of the strongly nonlinear dependence of h_c/t on L_s/S for smaller values of stiffener wall thickness, the material volume depends monotonically on L_s. As a result, over the range of parameters considered, the shortest stiffener analyzed ($L_s = 0.2S$) proved to be the most efficient buckle arrestor from the point of view of minimizing the weight of the structure.

In spite of differences in the mechanism of initiation of collapse in panels with higher values of λ (unsymmetric bifurcation buckling), similar analyses of the process of arrest of propagating buckles revealed no significant departures from the behavior described above. Results from such analyses can be found in Power (1995).

CONCLUSIONS

The paper revisits the subject of propagating collapse in long, shallow, pressure-loaded panels and addresses the issue of arrest of such collapse. It is demonstrated that circumferential stiffeners, periodically placed along the length of such panels, can accomplish this task. The traditional role of such stiffeners has been to increase the global buckling pressure of the structure. By contrast, in the present work, the stiffeners are cast in a buckle containment role where collapse, should it occur, is constrained to remain within the region bounded by two such stiffeners. A methodology has been presented for evaluating the effectiveness of circumferential stiffeners in this non-traditional application. The methodology is general enough so that it can form the basis of similar studies of arrest in other problems which can experience propagating instabilities.

In the present problem, the tool used to evaluate the arresting effectiveness of stiffeners is an analysis which simulates numerically the engagement of a stiffener by a buckle propagating quasi-statically in shallow, elastic panels. The main result of the simulation is the pressure required to penetrate the buckle through the stiffener (*crossover pressure*, P_x), whose dependence on the length and thickness of the stiffener was studied parametrically. The major steps of the arresting evaluation methodology developed and some of the major findings pertinent to the present problem are as follows.

- A buckle arresting efficiency was defined with zero efficiency representing an arrestor with crossover pressure equal to the propagation pressure of the panel, which is the lowest pressure at which such buckles will propagate, and 100% efficiency representing arrestors with crossover pressure equal to the global buckling pressure of the panel. This is a natural definition of maximum efficiency because crossover pressures in excess of P_C cannot be obtained due to incipient global collapse at this pressure.
- It was demonstrated that the wall thickness of buckle arrestors must exceed a minimum value h_{cm}, regardless of stiffener length, if they are to achieve an arresting efficiency of 100%. A stiffener with wall thickness equal to this bounding value was given the name of *minimum thickness stiffener*.

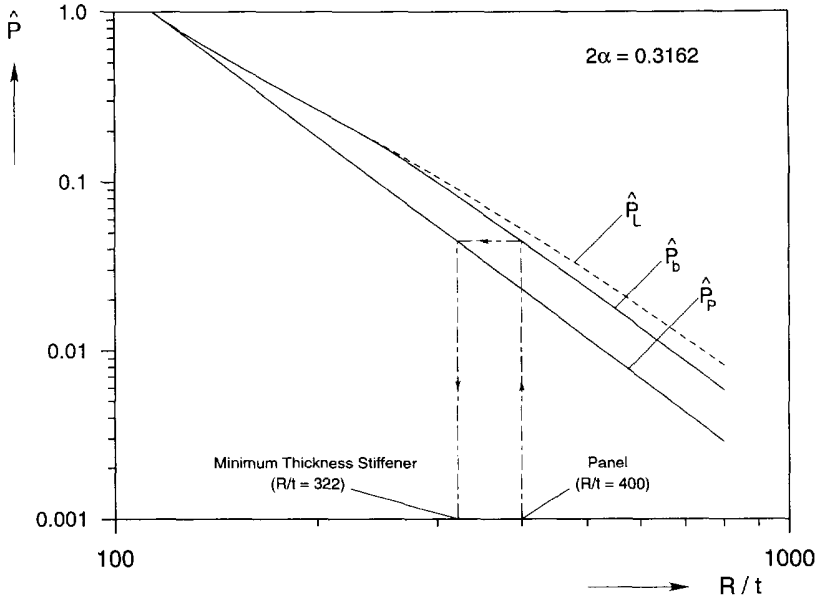

Fig. 11. Design of minimum thickness arrestors for panels with fixed span angle and various R/t values.

- The minimum thickness stiffener can be established with relatively modest effort as follows: Figure 11 shows a log-log plot of the critical buckling and propagation pressures for panels with a span angle of $2\alpha = 0.3162$ and R/t values ranging between 100 and 1000. In this figure, pressure is normalized by the propagation pressure of the most shallow panel in the family which exhibits snapthrough buckling, i.e., the one with $\lambda = 2.85$. We observe that for lower R/t values, global buckling is due to a limit load instability ($\hat{P}_L$), while panels with higher values of R/t experience bifurcation buckling ($\hat{P}_b$) (see Schreyer and Masur, 1966). The propagation pressure ($\hat{P}_P$) is evaluated from the closed form expression (2). As an example, consider a panel with $R/t = 400$. The minimum thickness arrestor for this panel is one whose propagation pressure is equal to the global buckling pressure of the panel. From the construction in the figure, this stiffener must therefore have $R/t = 322$. Since the stiffener and the panel have the same radius of curvature, this indicates that $h_{cm} = R/322$ for this case.
- For each stiffener thickness $h > h_{cm}$ there exists an arrestor of finite length with efficiency of 100%. The stiffener length required to produce such arrestors was established as a function of the stiffener thickness. For the problem and parameters considered in this paper, a minimum thickness stiffener with a length of just $L_{sm} = 1.8S$ produced an efficiency of 100%. As a result, any further increase in the length of this arrestor is unnecessary. Thus, well designed arrestors should have $h \geqslant h_{cm}$ and $L_s \leqslant L_{sm}$. The establishment of such limiting values of the two geometric variables of the problem will also be an essential first step in the design of such devices in other problems.
- For each stiffener thickness $h < h_{cm}$ there exists an arrestor length such that the arrestor appears to be infinitely long to an incoming propagating buckle. Increasing the arrestor length past this value results in no further increase in the crossover pressure of the arrestor. For the range of parameters studied, this length was not found to be strongly dependent upon stiffener thickness.
- The stiffener material volume is one of the problem design factors that must be considered. The stiffener length and wall thickness selected should tend to minimize the volume of material in the stiffener as well as provide adequate arresting performance. In the present problem, and for the range of parameters considered, the shortest critical thickness arrestor analyzed ($L_S = 0.2S$) is the one requiring the least material. This conclusion may not be applicable to other problems.

- An additional design issue is the spacing of such arresting devices. Clearly, this decision has to weigh the cost of the stiffeners against the potential cost of repairs to the length of structure damaged and must be made on a case-by-case basis.

Acknowledgement—The work was supported in part by the Office of Naval Research through grant N-00014-91-J-1103 and by the University of Texas at Austin.

REFERENCES

Chater, E. and Hutchinson, J. W. (1984). On the propagation of bulges and buckles. *ASME J. Appl. Mech.* **51,** 269–277.

Dyau, J. Y. and Kyriakides, S. (1993). On the localization of collapse in cylindrical shells under external pressure. *Int. J. Solids Structures* **30,** 463–482.

Ericksen, J. L. (1975). Equilibrium of bars. *J. Elasticity* **5,** 191–201.

Kyriakides, S. (1993). Propagating instabilities in structures. In *Advances in Applied Mechanics* (Edited by J. W. Hutchinson and T. Y. Wu) Vol. 30, pp. 67–189. Academic Press, Boston.

Kyriakides, S. and Arseculeratne, R. (1993). Propagating instabilities in long shallow panels. *ASCE J. Engng Mech.* **119,** 570–583.

Kyriakides, S. and Babcock, C. D. (1980). On the "slip-on" buckle arrestor for offshore pipelines. *ASME J. Pressure Vessel Tech.* **102,** 188–193.

Power, T. L. and Kyriakides, S. (1994). Localization and propagation of instabilities in long shallow panels under external pressure. *ASME J. Appl. Mech.* **61,** 755–763.

Power, T. L. (1995). Collapse of long shallow panels under external pressure: initiation, localization, propagation, and arrest. Ph.D. dissertation, Engineering Mechanics, The University of Texas at Austin, EMRL Report No. 95/3.

Riks, E. (1979). An incremental approach to the solution of snapping and buckling problems. *Int. J. Solids Structures* **15,** 529–551.

Sanders, J. L. (1963). Nonlinear theories for thin shells. *Quart. Appl. Math.* **21,** 21–63.

Schreyer, H. L. and Masur, E. F. (1966). Buckling of shallow arches. *ASCE J. Engng Mech. Div.* **92,** 1–19.

APPENDIX A: KINEMATICS

The following nonlinear shell kinematics (Sanders, 1963) which incorporate the assumption that membrane strains are small were used in the analysis:

$$
\begin{aligned}
E_{xx} &= u_{,x} + \tfrac{1}{2}[u_{,x}^2 + v_{,x}^2 + w_{,x}^2],\\
E_{\theta\theta} &= \frac{w + v_{,\theta}}{R} + \frac{1}{2}\left[\left(\frac{u_{,\theta}}{R}\right)^2 + \left(\frac{v_{,\theta} + w}{R}\right)^2 + \left(\frac{w_{,\theta} - v}{R}\right)^2\right],\\
E_{x\theta} &= \frac{1}{2}\left[\frac{u_{,\theta}}{R} + v_{,x} + u_{,x}\frac{u_{,\theta}}{R} + v_{,x}\frac{v_{,\theta} + w}{R} + w_{,x}\frac{w_{,\theta} - v}{R}\right],\\
K_{xx} &= -[u_{,xx}N_x + v_{,xx}N_\theta + w_{,xx}N_z],\\
K_{\theta\theta} &= -\left[\frac{u_{,\theta\theta}}{R^2}N_x + \frac{v_{,\theta\theta} + 2w_{,\theta} - v}{R^2}N_\theta + \frac{w_{,\theta\theta} - 2v_{,\theta} - w - R}{R^2}N_z + \frac{1}{R}\right],
\end{aligned}
\tag{A.1}
$$

and

$$
K_{x\theta} = -\left[\frac{u_{,x\theta}}{R}N_x + \frac{v_{,x\theta} + w_{,x}}{R}N_\theta + \frac{w_{,x\theta} - v_{,x}}{R}N_z\right].
$$

N_x, N_θ, and N_z are the components of the normal to the deformed panel midsurface given by:

$$
\begin{aligned}
N_x &\cong v_{,x}\frac{w_{,\theta} - v}{R} - w_{,x}\frac{w + v_{,\theta}}{R} - w_{,x},\\
N_\theta &\cong w_{,x}\frac{u_{,\theta}}{R} - u_{,x}\frac{w_{,\theta} - v}{R} - \frac{w_{,\theta} - v}{R},
\end{aligned}
\tag{A.2}
$$

and

$$
N_z \cong 1 + u_{,x} + \frac{w + v_{,\theta}}{R} + u_{,x}\frac{w + v_{,\theta}}{R} - v_{,x}\frac{u_{,\theta}}{R}.
$$